Poisson-Nernst-Planck Equations for Simulating Biomolecular Diffusion-Reaction Processes II: Size Effects on Ionic Distributions and Diffusion-Reaction Rates

Benzhuo Lu[†*] and Y. C. Zhou[‡]

[†]State Key Laboratory of Scientific and Engineering Computing, Institute of Computational Mathematics and Scientific/Engineering Computing, Academy of Mathematics and Systems Science, Chinese Academy of Sciences, Beijing, China; and [‡]Department of Mathematics, Colorado State University, Fort Collins, Colorado

ABSTRACT The effects of finite particle size on electrostatics, density profiles, and diffusion have been a long existing topic in the study of ionic solution. The previous size-modified Poisson-Boltzmann and Poisson-Nernst-Planck models are revisited in this article. In contrast to many previous works that can only treat particle species with a single uniform size or two sizes, we generalize the Borukhov model to obtain a size-modified Poisson-Nernst-Planck (SMPNP) model that is able to treat nonuniform particle sizes. The numerical tractability of the model is demonstrated as well. The main contributions of this study are as follows. 1), We show that an (arbitrarily) size-modified PB model is indeed implied by the SMPNP equations under certain boundary/interface conditions, and can be reproduced through numerical solutions of the SMPNP. 2), The size effects in the SMPNP effectively reduce the densities of highly concentrated counterions around the biomolecule. 3), The SMPNP is applied to the diffusion-reaction process for the first time, to our knowledge. In the case of low substrate density near the enzyme reactive site, it is observed that the rate coefficients predicted by SMPNP model are considerably larger than those by the PNP model, suggesting both ions and substrates are subject to finite size effects. 4), An accurate finite element method and a convergent Gummel iteration are developed for the numerical solution of the completely coupled nonlinear system of SMPNP equations.

INTRODUCTION

Ionic solutions do not resemble an ideal solution or perfect gas of noninteracting uncharged particles. Indeed, ions such as Na^+ and K^+ have specific properties, and can be selected by biological systems, because they are nonideal and have highly correlated behavior. Screening and finite size effects produce the correlations more than anything else (1). The nonideality of ionic solutions is a central subject in many electrochemistry textbooks (2–5). Poisson-Boltzmann (PB) theory for screening has been an established, mathematically well analyzed, and numerically tractable model for describing the equilibrium state of ionic solution systems. Typical applications of PB theory include solvated macromolecule-solvent-mobile ion systems in molecular biophysics, electrolyte and electrode systems in electrochemistry, or the interactions between an interface and the colloid solution.

Despite the wide applicability of the traditional PB theory, limitations due to the underlying mean-field approximation are recognized, and discrepancies in the predicted ionic concentration profile from experiments (6,7) and simulations (8) are observed. These situations usually involve large potentials ($>>kT/e$) that can be found in many real applications. The large potential/voltage can be induced either by large surface charge (as of electrode) or highly charged biomolecules such as nucleic acids. Because solvated ions are treated as point charges in the standard mean-field assumption and ion-ion correlations are neglected (except for screening by ionic atmosphere), the ion concentrations predicted by the Boltzmann distribution $e^{-\beta q\phi}$ can approach infinity with the increasing electric potential. Such a scenario is nonphysical, as an ionic saturation will be established because of the steric exclusion among ions.

There are many standard review articles and monographs on the finite size effects, among which Pitzer, for example, summarizes the life's work of a generation of electrochemists interested in these effects (5,9–16). To incorporate the effects of finite particle sizes in the study of ionic solutions, most efforts are made through including exclusion terms from liquid-state theory or density functional theory (DFT) (17–29). The work by Evans (30), Roth et al. (31), Hansen-Goos and Roth (32), Rosenfeld (33), and Roth (34) are built on the DFT of uncharged solutions. These theories are particularly important in understanding the main experimental properties of ionic solutions (see Kunz and Neueder (35) for a summary). However, the improvements of these new models over the traditional PB theory are somehow limited due to the intrinsic complexity of the models, the difficulties in mathematical analysis, numerical computation, and practical implementations.

For instance, coupling PNP and DFT usually invokes integral-differential equations, the numerical implementation of which on real biomolecular simulations can be

Submitted December 28, 2010, and accepted for publication March 31, 2011.

*Correspondence: bzlu@lsec.cc.ac.cn

Editor: Nathan Andrew Baker.

0006-3495/11/05/2475/11 $2.00

doi: 10.1016/j.bpj.2011.03.059

highly involved. Among these theories, the Borukhov model that follows the early work of Eigen and Wicke (36), and Kraljiglic and Iglic (19) appears attractive because it captures basic size effects by using a simplified formulation. The Borukhov model modifies the free energy functional of the ionic system (mean-field approximation) by adding an ideal-gas-like solvent entropy term. This term represents the unfavorable energy that models the over-packing or crowding of the ions and solvent molecules, and thus the steric effects are taken into account in the model.

The Borukhov free energy form treats all ion species and solvent molecules with an identical size, and a modified PBE (MPB) can be derived through the minimization of the free energy. Although this model, hereby referred to the free energy functional model, can be in principle extended to account for different sizes of ions and solvent molecules, general explicit expressions for ionic concentrations as functions of the potential and particle sizes have not been derived. Such a general expression of charge density is needed to supply the Poisson equation to obtain the final MPB equation. A recent extension of the Borukhov model is able to treat particle species of two sizes, and the resulting MPB does not add much difficulty to a normal PB solver in the numerical solution (24). For systems with three or more different particle sizes, however, the method becomes prohibitively tedious if one wants to get the ionic concentrations as functions of potential and particle sizes, although implicit relations can be derived.

To avoid the above difficulty, we will try not to find the explicit form of the size-modified PB equation and its solution. Considering the fact that the PB/MPB solution (corresponding to the equilibrium description of electrolyte) is merely a stationary point of the free energy functional of the system, we will instead solve an energy minimization problem through evolution of the energy system. This naturally corresponds to the physical evolution process of a nonequilibrium system in which nonzero ionic flux exists (i.e., detailed balance is broken). When coupled with electrostatics, such processes are usually described as electro-diffusion. The Poisson-Nernst-Planck equations (PNP) or the variants are established models in this field. Solutions of the PNP equations provide not only the description of the equilibrium state but also the dynamic information.

In biophysics, the PNP model is usually applied to ion channel studies; however, for one of our interests in this work it will be used to calculate the reaction rates of diffusion-reaction processes for enzyme-substrate systems. A developed theory called PNP/DFT combines finite size effects and the PNP theory (27–29). The biological implications of these effects are profound, as Nonner, Eisenberg, and their collaborators have shown how finite size effects produce selectivity in several types of channels (1,37–40) (B. Eisenberg, unpublished). In this work, we will start with the Borukhov model to derive a system of partial differential equations without incurring integral equations. These partial differential equations can be numerically solved at a practically tolerable efficiency for three-dimensional real molecular systems. We note that a modified PNP based on the Borukhov model was recently adopted to numerically investigate the size effects and dynamic properties of a one-dimensional diffusion system (25).

This article is dedicated to the generalization of the Borukhov model to treat ionic solution systems that:

1. have particle species of arbitrarily different sizes (ions, solvent molecule, and substrate molecule) and
2. exist in both equilibrium and nonequilibrium states.

We will revisit and compare some other size-modified Poisson-Boltzmann and Poisson-Nernst-Planck models. Particular attention will be paid to the size effects on the diffusion-reaction rate coefficients. The generalization of the Borukhov model results in a new size-modified PNP (SMPNP) model (42).

A finite element method is described for solving the three-dimensional SMPNP system, and the numerical tractability of the SMPNP model is demonstrated. We arrive at two major conclusions:

1. A size-modified PB model is essentially reproduced in the numerical solution of the SMPNP model. This general PB model can be regarded as a special case of the SMPNP by equipping the PNP equations with proper boundary and interface conditions (i.e., vanishing flux at the interface/boundary; see Methods).
2. Under proper boundary conditions, the SMPNP equations enable us to study more-general diffusion processes (e.g., to study diffusion-reaction with a reactive boundary/interface). The size effects will be shown by the variation of the diffusion-controlled reaction rate, and by the modification of the substrate and ionic concentrations as well as the electric field.

METHODS

PNP continuum model

For an ionic solution, we use p_i to denote the density of the i^{th} species ions, and use ϕ to denote the electrostatic potential. Given a free energy form $F(p, \phi)$ of the ionic solution, where p denotes the collection of p_i, a continuum model (equations) can be derived to describe the coupling between the charged particle diffusion and the electrostatics by using the constitutive relations about the flux and the electrochemical potential μ_i of the i^{th} species

$$J_i = -m_i p_i \nabla \mu_i. \tag{1}$$

Here m_i is the ion mobility that relates to its diffusivity D_i through Einstein's relation $D_i = m_i k_B T$, where k_B is the Boltzmann constant and T is temperature. Define μ_i to be the variation of F with respect to p_i:

$$\mu_i = \frac{\delta F}{\delta p_i}, \tag{2}$$

then the transport equations are obtained from the mass and current conservation law

$$\frac{\partial p_i}{\partial t} = -\nabla J_i. \tag{3}$$

These, together with a Poisson equation describing the electrostatic field, form a full PNP equation system.

The traditional mean-field free energy form $F(p, \phi)$ with the ionic size-exclusion and correlation effects neglected leads to the PNP equations (see the following subsections). The interests of this article focus on the applications to solvated biomolecular systems with two distinguished domains—one occupied by the biomolecule(s), and the other by the ionic solution. Here we consider only the steady state (can be either in equilibrium or in nonequilibrium with steady flow), i.e., $\partial p_i/\partial t = 0$. The PNP equations for such a system with K ion species are (43)

$$\nabla\,[Di(r)\,\nabla pi(r,\,t) + \beta\,Di(r)p_i(r,\,t)q_i\,\nabla\phi(r)] = 0, \quad r \in \Omega_s,\ i = 1\ldots K, \tag{4}$$

$$-\nabla \cdot \varepsilon(r)\nabla\phi(r,t) - \rho^f(r) - \lambda\sum_i q_i p_i(r,t) = 0, \quad r \in \Omega, \tag{5}$$

where $\beta = 1/k_BT$, q_i is the charge of each particle of species i. The value $\rho^f(r)$ is the fixed charges of the biomolecule, λ equal to 1 in Ω_s and 0 in the molecule region Ω_m because the diffusive particle does not penetrate into the solvent domain Ω_m. A two-dimensional schematic illustration is shown in Fig. 1. We want to solve Eqs. 4 and 5 to get the density p and potential ϕ.

Review of the Borukhov model

The standard PNP equations ignore the important effects of the finite size of ions, thought to be the predominant factor in determining the nonideal properties of ionic solutions (1–3,5,9). This work intends to develop a simple finite size model that can be numerically solved for real systems, by possibly employing the finite element framework built in our former work (44). A simple model in this article means one that can be described with differential equation(s) alone, rather than one that must be described by using differential-integral equation(s) or other complex forms. Our study shows that even the standard PNP model, although free of any size effect, is not trivial in the matter of obtaining a numerical solution for actual large biomolecular systems (43,44). To model the effects of the ion size on the electrostatics and ion distributions in electro-physiological systems, Borukhov et al. (22) considered a free energy functional for 1:z asymmetric electrolyte of two ion species. Both ion species and the solvent molecules are assumed to have the same effective size a^3. The grand canonical free energy functional in terms of electrostatic potential $\phi(r)$ and ion concentrations $p_+(r)$ and $p_-(r)$ are given by

$$F = U - TS - V, \tag{6}$$

where U is internal energy, S is entropy, T is absolute temperature, and V is the chemical potential:

$$U = \int\left[-\frac{\varepsilon}{2}|\nabla\phi|^2 + ep_+\phi - zep_-\phi\right]dr, \tag{7}$$

$$-TS = \frac{k_BT}{a^3}\int\left[p_+a^3\ln\left(p_+a^3\right) + p_-a^3\ln\left(p_-a^3\right) + \left(1 - p_+a^3 - p_-a^3\right)\ln\left(1 - p_+a^3 - p_-a^3\right)\right]dr, \tag{8}$$

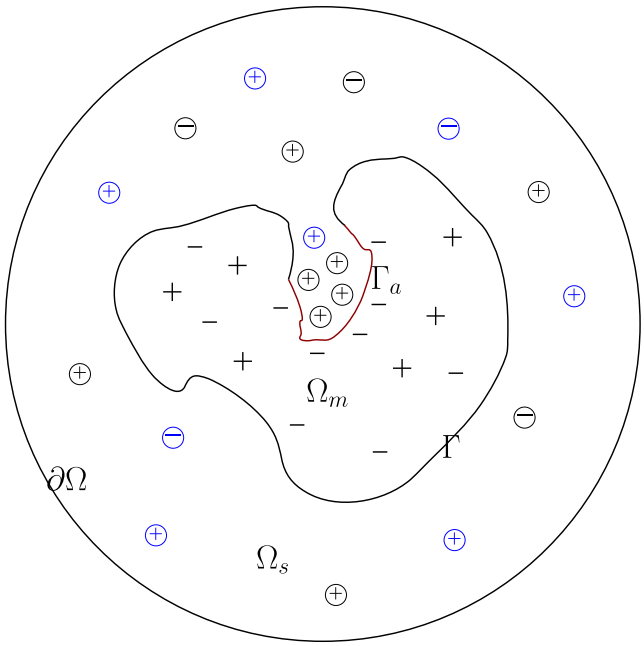

FIGURE 1 Two-dimensional schematic illustration of the computational domain modeling a solvated biomolecular system. The biomolecule(s) is located in domain Ω_m and the aqueous solution is in domain Ω_s. The molecular surface is Γ. The active reaction center $\Gamma_a \subset \Gamma$ is highlighted in red. The circles of different colors with plus or minus sign inside represent the diffusive charged particles of different species that have finite sizes and move only in Ω_s. The singular charges inside molecules are signified with plus or minus sign in Ω_m. The minimum distance between the molecular surface Γ and the exterior boundary $\partial\Omega$ is much larger than the diameter of the molecule so that approximate boundary condition for the electrostatics can be applied.

$$V = \int(\mu_+p_+ + \mu_-p_-)\,dr. \tag{9}$$

The third entropy term introduces the solvent density

$$\frac{1}{a^3}\left(1 - p_+a^3 - p_-a^3\right)$$

to account for the solvent entropy, provided that the ions and solvent molecules are compactly packed. The steric exclusion effect is implied because the ionic density is prevented from going beyond $1/a^3$ (the solvent density should be no less than zero). If this term is dropped, the functional in Eq. 6 will degenerate into the traditional free energy form that eventually leads to the standard PB or PNP (see the following subsections).

The chemical potential μ_i can be regarded as a Lagrange multiplier that represents the constraint on the total number of ion particles. Following the method in Lu et al. (44), one more Lagrange multiplier can be introduced and an associated term, the electrostatic potential $\phi\,(r)$, can also be regarded as an independent field. The extremization of F with respect to ϕ gives the Poisson equation. An alternative treatment is to simply add the Poisson equation

$$\nabla^2\phi = -\frac{1}{\varepsilon}[ep_+ - zep_-] \tag{10}$$

as an additional constraint to the system. After applying the extrema conditions

$$\frac{\delta F}{\delta p_+} = 0 \text{ and } \frac{\delta F}{\delta p_-} = 0,$$

the following equalities hold true:

$$e\phi - \mu_+ + \frac{k_B T}{a^3}\left[a^3 \ln\left(p_+ a^3\right) - a^3 \ln\left(1 - p_+ a^3 - p_- a^3\right)\right] = 0, \tag{11}$$

$$\begin{aligned} &- ze\phi - \mu_- + \frac{k_B T}{a^3}\left[a^3 \ln\left(p_- a^3\right)\right. \\ &\left. - a^3 \ln\left(1 - p_+ a^3 - p_- a^3\right)\right] = 0. \end{aligned} \tag{12}$$

Subtracting Eq. 12 from 11, we get

$$p_+ = p_- e^{\beta(\mu_+ - \mu_-) - \beta(1+z)e\phi}. \tag{13}$$

The potential ϕ is weak in the region far away from the molecules, and thus the positive and negative ion densities approach their respective bulk densities p_{+b} and p_{-b}. This suggests that the electroneutrality will be a reasonable assumption, i.e., $p_{+b} = zp_{-b} = zp_b$ (assuming $p_{-b} = p_b$). As a result,

$$e^{\beta(\mu_+ - \mu_-)} = z, \tag{14}$$

and thus

$$p_+ = zp_- e^{-\beta(1+z)e\phi}. \tag{15}$$

Plug Eq. 15 into Eqs. 11 and 12, and we get

$$\frac{p_+ a^3}{1 - p_+ a^3 - p_- a^3} = e^{\beta(\mu_+ - e\phi)}, \tag{16}$$

$$\frac{p_- a^3}{1 - zp_- a^3 e^{-\beta(1+z)e\phi} - p_- a^3} = e^{\beta(\mu_- + ze\phi)} = \frac{1}{e^{-\beta\mu_-} e^{-z\beta e\phi}}. \tag{17}$$

Hence,

$$p_- = \frac{1}{a^3} \frac{1}{1 + e^{-\beta\mu_-} e^{-z\beta e\phi} + ze^{-\beta(1+z)e\phi}}. \tag{18}$$

A comparison of Eq. 18 with Eq. 12 when $p_- \to p_b$ as $\phi \to 0$ gives

$$\frac{p_b a^3}{1 - (1+z)p_b a^3} = e^{\beta\mu_-}. \tag{19}$$

Note that when the size effect is considered, the usual identity, $p_b = 1/a^3\, e^{\beta\mu}$, no longer holds.

Substitute Eq. 19 into 18, and we get

$$p_- = \frac{c_b e^{\beta z e\phi}}{1 - v_0 + v_0(e^{z\beta e\phi} + ze^{-\beta e\phi})/(1+z)}, \tag{20}$$

where $v_0 = (1+z)a^3 p_b$ is the total bulk volume fraction of the positive and negative ions, and

$$p_+ = \frac{zc_b e^{-\beta e\phi}}{1 - v_0 + v_0(e^{z\beta e\phi} + ze^{-\beta e\phi})/(1+z)}. \tag{21}$$

Finally, the MPB equation is given as

$$\nabla^2\phi = \frac{zep_b}{\varepsilon} \frac{e^{\beta z e\phi} - e^{-\beta e\phi}}{1 - v_0 + v_0(e^{\beta z e\phi} + ze^{-\beta e\phi})/(1+z)}. \tag{22}$$

It can be seen that in zero size limit ($a \to 0$) or dilute limit ($p_b \to 0$, hence $v_0 \to 0$), the Eqs. 20–22 are reduced to the PBE. As aforementioned, the closed-form expressions (explicit functions) of ionic densities are essential for deriving the final MPB equation. This can be achieved by assuming a uniform size for all the positive and negative ions and solvent molecules. Recently, Chu et al. (24) extended the Borukhov model to the case with two different sizes, and they showed that the resulting MPB did not create significant extra difficulties to a normal PB solver in the numerical solution. Chu's approach is based on the lattice model for two large ionic species with a same diameter a and one small species with a diameter a/k for some integer number k. If the system has three or more different particle sizes, it becomes prohibitively tedious to follow that approach to derive the ionic densities as functions of potential and particle sizes.

On the other hand, although an MPB equation cannot be explicitly derived when particle sizes in the functional Eq. 8 are nonuniform, the ion densities are still determined by the particle size and the electric potential albeit implicitly. This fact is also recognized in the literature (45–47).

In the following, we plan to directly work on the size-modified PNP equation systems that are derived from the free energy functional with arbitrarily different particle sizes. From there, we will show that a SMPB model is implied in the SMPNP model, and this implication can be numerically tracked from solutions of the SMPNP equations under specific boundary/interface conditions. Our approach avoids the difficulties and complexities in the derivation of an explicit MPB mode with different sizes. An additional asset of PNP/SMPNP model is its wider applications to nonequilibrium studies.

Phenomenological model of electro-diffusion with finite particle sizes

According to the classical fluid density functional theory, the free energy of an ionic solution system can be written as (e.g., see (45))

$$F = k_B T \int \left[\sum_i p_i \left(\ln\left(\frac{p_i}{\zeta_i}\right) - 1\right)\right] dx + F_{ex}(p) + F_{ext}, \tag{23}$$

where the summation is taken over the total K ion species. The first term is the ideal gas component, F_{ex} is the excess free energy functional, F_{ext} is the term representing the contribution of the external interaction, and ζ_i is the fugacity of the i^{th} particle species (ion or solvent molecule). For ideal gas, the fugacity is equal to the density,

$$\zeta_i = p_{ib} = \frac{1}{a_i^3},$$

where a_i is the effective size. For free energies of a more general nature, different relations may exist between the fugacity and respective bulk density of each particle species. As we will show later, these constants $\{\zeta_i\}$ will not alter the SMPB or SMPNP models finally derived. To connect our SMPNP mode to the previous SMPB model, we assign ζ_i the approximate values of ideal gas. Similarly, for a solvent molecule with effective size a_0 and pure solvent density p_0, its fugacity takes a value of

$$\zeta_i = p_0 = \frac{1}{a_0^3}.$$

Such a value is equivalent to assuming a zero chemical potential, $\mu_0 = k_B T \ln(p_0 a_0^3) = 0$, for the pure solvent (reference state). If we ignore F_{ext} in our biomolecular system and consider only the electrostatic interaction in F_{ex} in addition to the solvent entropy term as in Borukhov model, a generalized free energy

$$F = \int \frac{1}{2}\Big[\rho^f + \lambda \sum_i z_i e p_i\Big]\phi dx + k_B T \int \Big[\sum_i p_i\big(\ln\left(p_i a_i^3\right) - 1\big) + p_0\Big(1 - \sum_i p_i a_i^3\Big)\ln\Big(p_0\Big(1 - \sum_i p_i a_i^3\Big)a_0^3 - 1\Big)\Big]\, dx, \tag{24}$$

is obtained, where z_i values are the valence of i^{th} ion species.

Let μ_i be the variation of F with respect to p_i, i.e.,

$$\begin{aligned}\mu_i &= \frac{\delta F}{\delta p_i} = z_i e\phi + k_B T\Big[\ln\left(p_i a_i^3\right) - p_0 a_i^3 \ln\Big(p_0\Big(1 - \sum_i p_i a_i^3\Big)\, a_0^3\Big)\Big] \\ &= z_i e\phi + k_B T\Big[\ln\left(p_i a_i^3\right) - k_i \ln\Big(1 - \sum_i p_i a_i^3\Big)\Big],\end{aligned} \tag{25}$$

where $k_i = a_i^3/{a_0}^3$.

Using the electroneutrality condition we will get the relation between μ_i and p_{ib} at $\phi = 0$:

$$\begin{aligned}\mu_i &= \frac{\delta F}{\delta p_i}|_{\phi=0} = k_B T\Big[\ln\left(p_{ib} a_i^3\right) - k_i \ln\Big(1 - \sum_l p_{lb} a_l^3\Big)\Big] \\ &= k_B T \ln \frac{p_{ib} a_i^3}{\Big(1 - \sum_l p_{lb} a_l^3\Big)^{k_i}}.\end{aligned} \tag{26}$$

In the case of two ion species, when $k_1 = k_2 = 1$, Eqs. 25 and 26 provide the density expressions in the Borukhov model for a general asymmetric electrolyte.

Comparison with the two-size SMPB model

We now look at the relationship between our new formulation and Chu's SMPB method that can treat two different sizes (24). In that article, they consider three ion species in which two species have a larger identical size a and one has a smaller size a/k. The k can be any real value, and is chosen to be an integer so that the lattice-gas theory can be readily applied. In the comparison, we consider two ion species with sizes $a_1 \neq a_2$ without loss of the essential of their approach.

For two ion species, at $\phi = 0$, Eq. 26 gives

$$\mu_1 = k_B T \ln \frac{p_{1b} a_1^3}{\Big(1 - \sum_i p_{ib} a_i^3\Big)^{k_1}}, \tag{27}$$

$$\mu_2 = k_B T \ln \frac{p_{2b} a_2^3}{\Big(1 - \sum_i p_{ib} a_i^3\Big)^{k_2}}, \tag{28}$$

where $k_1 = a_1^3/a_0^3$, $k_2 = a_2^3/a_0^3$, and a_0 is the solvent molecule size. The sizes a_1 and a_2 can be arbitrary, and are not necessarily larger than the solvent molecule size a_0.

Using the lattice-gas method as in the work of Chu et al. (24), supposing the bigger size is $a_2 = a$, the smaller size $a_1 = a/k$, the grand partition function for each lattice site (enumerating all possible occupancies of the lattice site of total N) is given by

$$z = \left(1 + e^{\beta(\mu_1 - z_1 e\phi)}\right)^k + e^{\beta(\mu_2 - z_2 e\phi)}. \tag{29}$$

The relationship between the bulk density p_{ib} and the chemical potential μ_i is obtained by considering the grand partition function with respect to the chemical potential for $\phi = 0$,

$$p_{ib} = \frac{k_B T}{N a^3} \frac{\partial \ln z^N}{\partial \mu_i}\Big|_{\phi=0}. \tag{30}$$

They thus give

$$\begin{aligned}p_{1b} &= \frac{k_B T}{a^3} \frac{1}{\left(1 + e^{\beta\mu_1}\right)^k + e^{\beta\mu_2}} k\left(1 + e^{\beta\mu_1}\right)^{k-1} \beta e^{\beta\mu_1}, \\ p_{2b} &= \frac{k_B T}{a^3} \frac{1}{\left(1 + e^{\beta\mu_1}\right)^k + e^{\beta\mu_2}} \beta e^{\beta\mu_2}.\end{aligned}$$

But then

$$\begin{aligned}\mu_1 &= k_B T \ln \frac{p_{1b} a_1^3}{1 - p_{2b} a^3 - p_{1b} a^3/k}, \\ &= k_B T \ln \frac{p_{1b} a_1^3}{1 - \sum_i p_{ib} a_i^3},\end{aligned} \tag{31}$$

$$\mu_2 = k_B T \ln \frac{p_{2b} a_2^3}{1 - \sum_i p_{ib} a_i^3}. \tag{32}$$

Comparing Eqs. 27 and 28 with Eqs. 31 and 32, it is found that the chemical potentials in the work of Chu et al. (24) are similar to our PNP model except for a factor k_i (the power of volume faction) in the logarithm as shown in Eqs. 27 and 28. In the case of identical sizes, i.e., $k_1 = k_2 = 1$, the two models give the same result.

The final SMPNP model

Plug Eq. 25 into Eqs. 1–3, and we now get

$$\begin{aligned}\frac{\partial p_i}{\partial t} &= -\nabla \cdot J_i = \nabla \cdot (m_i p_i \nabla \mu_i) \\ &= \nabla \cdot D_i \left(\nabla p_i + \frac{k_i p_i \sum_l a_l^3 \nabla p_l}{1 - \sum_l a_l{}^3 p_l} + \beta p_i z_i e \nabla\phi\right).\end{aligned} \tag{33}$$

Together with the Poisson equation, we get our final SMPNP model (steady state),

$$-\nabla \cdot D_i(r)\left[\nabla p_i(r) + \frac{k_i p_i(r)}{1 - \sum_l a_l^3\, p_l(r)} \sum_l a_l^3 \nabla p_l(r) + \beta p_i(r) q_i \nabla\phi(r)\right] = 0, \quad r \in \Omega_s, \tag{34}$$

$$-\nabla \cdot \varepsilon(r)\nabla\phi(r,t) - \rho^f(r) - \lambda \sum_i q_i\, p_i(r,t) = 0, \quad r \in \Omega, \tag{35}$$

where $q_i = z_i e$ is the charge of i^{th} species with $1 \le i \le K$. We want to solve Eqs. 34 and 35 to get the density p_i and electrostatic potential ϕ.

It can be shown that when all the sizes a_i are equal, the above SMPNP model is simply the Borukhov free energy expression and the modified PBE (22), and is also the modified PNP in Kilic et al. (25). For the case

of two ion sizes, it gives a very close but different form of the size-modified Poisson-Boltzmann equation in Chu et al. (24).

A symmetrically transformed form of the SMPNPEs

As studied in previous works (43,44), the standard Nernst-Planck equations (NPEs) from Eq. 4 can be transformed into a symmetric form

$$\frac{\partial(\overline{p}_i e^{-\beta q_i \phi})}{\partial t} = \nabla \cdot (\overline{D}_i \nabla \overline{p}_i) \tag{36}$$

by introducing the transformed variables

$$\begin{aligned} \overline{D}_i &= D_i e^{-\beta q_i \phi}, \\ \overline{p}_i &= p_i e^{\beta q_i \phi}. \end{aligned} \tag{37}$$

Similarly, a pro forma form of the SMNPEs Eq. 34 can also be written as

$$\frac{\partial(\overline{p}_i e^{-\beta V_i})}{\partial t} = \nabla \cdot (\overline{D}_i \nabla \overline{p}_i), \tag{38}$$

with

$$\begin{aligned} V_i &= q_i \phi - \frac{k_i}{\beta} \ln\left(1 - \sum_l^K a_l^3 p_l\right), \\ \overline{D}_i &= D_i e^{-\beta V_i}, \\ \overline{p}_i &= p_i e^{\beta V_i}. \end{aligned} \tag{39}$$

Physically, V_i can be seen as a modification of the potential ϕ due to consideration of the size effects in the SMPNP model.

However, it is worth noting that, in the traditional PNP, $\overline{D}$ is only dependent on ϕ, but not on p. Therefore, for a given ϕ, the stiffness matrices of Eq. 36 are symmetric, whereas, in Eq. 39 for the SMPNP, the coefficient $\overline{D}_i$ depends on both ϕ and the unknown p_i. This coupling will lead to different properties of the transformed SM NPEs (Eq. 38) from that of the transformed NP Eq. 36. In the numerical solution by iterations as described in the Methods, one can use the solution of p^{n-1} at n-1$^{\text{th}}$ step solution to calculate the coefficient $\overline{D}$, and then solve the transformed SM NP Eq. 38 to obtain the solution of p^n at the current n^{th} step. This strategy could make the stiffness matrices symmetric in numerical implementations. The numerical properties of such a strategy has not been studied yet, and we will not adopt that strategy in this article for the reasons mentioned below.

The transformation equations, Eqs. 36 and 37, are also frequently used in solving the PNP equations for semiconductor device simulations (48,49). It is anticipated that the discretization in solving the transformed Eq. 36 could produce a stiffness matrix with a smaller condition number compared to the original Eq. 4 with a nonsymmetric elliptic operator, and thus iterative methods applied to the linear system might converge faster. However, in the biomolecular case, as shown by our study, the transformed formulation is actually always related to a large condition number of the stiffness matrix, due to the presence of a strong electrostatic field near the molecular surface (44).

For this reason, we will not explore the numerical properties in solution of the transformed SMPNPEs in this work. However, in some cases, the transformed SMPNPEs might be useful. For instance, the Slotboom variables are associated with the weighted inner product in many finite element approximations of semiconductor NP equations (50), for which exponential fitting techniques are usually used to obtain numerical solutions free of nonphysical spurious oscillations. Although the solutions in our numerical experiments and biophysical applications presented below do not show significant nonphysical oscillations, these methods can be adopted if needed.

Numerical implementation

The numerical properties and implementation of the SMPNPEs can be seen in the Supporting Material.

How to get SMPB results from the solution of the SMPNPEs

To obtain SMPB results, we can solve the SMPNPEs with asymmetric ion sizes as expected for the SMPBE calculation. We would use similar boundary conditions as in the usual solution of the PBE for ϕ, such as $\phi = 0$ or the Debye-Hückel approximation at the outer boundary $\partial\Omega$, and using the ionic bulk densities as boundary conditions for p_i. In addition, we use a reflective condition for each ion species in the molecular interface Γ (no Γ_a for PB calculation) to enforce zero-flux across the interface

$$J(r)_i = 0, \quad r \in \Gamma.$$

Then, the solution leads to the SMPB results. The reason is as follows: From Subsection S1.1 in the Supporting Material, we know that the SMPNPEs system has only one solution, and we also know that the solution of zero-flux-everywhere $J_i = 0$ (equilibrium) is a solution of the SMPNP system, which corresponds to the special case of the SMPB model. The equilibrium distribution can be explicitly seen from the PNP situation (see Eqs. 1 and 4) in which the zero-flux condition at boundary Γ

$$J_i = D_i(r)(\nabla p_i(r, t) + \beta p_i(r, t) q_i \nabla \phi(r)) = 0$$

can be seen equivalent to the Boltzmann distribution condition

$$p_i = p_{bi} e^{-\beta z_i e \phi}.$$

In SMPNP, the equilibrium distribution is also implicitly determined by $J_i = 0$, although a closed-form Boltzmann-like distribution is not available in general. Therefore, the SMPNP solution obtained from the above procedure with zero-flux conditions at Γ must satisfy the zero-flux condition everywhere. This indicates that the solution of SMPNP is exactly the solution of the SMPBE. This equivalence is numerically proven true for the standard PBE and PNPE system in our previous work on PNP (43), where it was shown that PBE and PNPE have essentially the same results despite a small numerical error.

RESULTS AND DISCUSSIONS

The following numerical tests are performed on a sphere model. These tests capture the fundamental difference between SMPB/SMPNP models and the classical PB/PNP models. In the sphere model, a unit sphere with a positive unit charge in the center simulates the solute molecule. When solving the PNP or SMPNP with a reactive substrate species, the entire surface of the sphere serves as the reactive boundary Γ_a. The exterior boundary of the computational domain is the concentric sphere of radius 40 Å.

Size effects on ionic concentrations in SMPB model

As analyzed in the above sections, an SMPB model is inherently contained in the SMPNP model. We will first investigate the size effects, in regard to the electrostatic potential and the ionic density distributions in the equilibrium state. Fig. 2 shows the ionic density profile in the SMPB model through solving the SMPNP equations with the boundary conditions described in Numerical Implication, below. The counterion densities that are at the similar order of the bulk water density are effectively reduced in the highly concentrated regions compared with the traditional PB

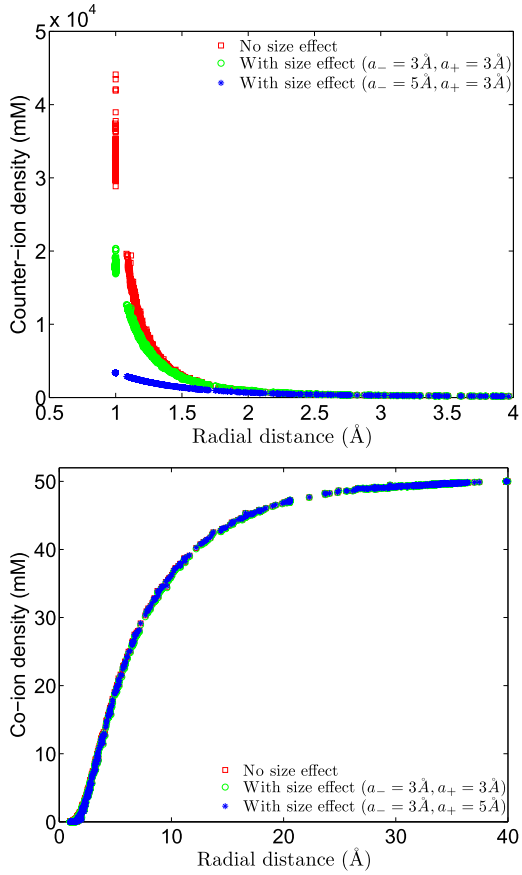

FIGURE 2 Counterion and coion densities in 1:1 salt around a unit sphere predicted by the PBE and the SMPBE (through SMPNPEs). a_- and a_+ are counterion size and coion size, respectively. The solvent molecular size is 2.5 Å. The ionic bulk densities are 50 mM.

predictions, which phenomena has also been demonstrated in the previous size-modified PB model. Although the coion density is not very sensitive to the size effects due to its small density ($\sim e^{-\beta e\phi}$, ϕ ~4 kcal/mol/e), which does allow more spacial area for its movement, the volume exclusion under such a circumstance is not very high.

Diffusion-reaction study with SMPNP model

The diffusion-controlled reactions in biomolecular systems can be investigated by using continuum approaches such as the PNP model (43), and the present SMPNP model. Three ion species are usually considered: the ion and counterion species accounting for the ionic strength of the solution; and the reactive particle species, as, for example, the substrates to be hydrolyzed by the enzyme (the biomolecule in the model). The densities of the first two species are given by p_1, and p_2, and the third given by p_3. Electroneutrality conditions demands that $p_{1b} + p_{2b} + p_{3b} = 0$. When solving the NPEs or SM NPEs, the homogeneous Neumann boundary condition is adopted for those species that have no reactions at the whole molecular surface. An (ideal) sink boundary condition $p_3 = 0$ is applied on Γ_a (representing the reactive site) for p_3. The reaction rate coefficient is defined as

$$k = \frac{\int_{\Gamma_a} J_3 \cdot ds}{p_{b3}}.$$

Without considering the size effects, the rate coefficient is also shown to be dependent on the substrate concentration (see Section S2 in the Supporting Material).

Size effects on the rate coefficient and the density profiles

Because of the intrinsic interactions among the densities of different ion species and the electric field, inclusion of the finite size effects of the mobile ions and substrate into the SMPNP model will change particle (ion and substrate) distributions and the electric field around the enzyme molecule, both of which consequently contribute to a modified reaction rate. As to be shown below, the rate change is mainly attributed to the direct variation of the gradient of substrate density, which itself is also influenced by the ionic size effects through regulating the overall electric field. The following illustrations indicate that the size effects may lead to a significant influence on the predicted reaction rates.

It is known that the diffusion coefficient of a particle depends on its size and shape, although such a dependence is not the topic of this work. Our concern here is the difference in the predicted reaction rates by the SMPNP and PNP models for a given diffusion coefficient that is known or measured experimentally. To concentrate on the diffusive particle size effect compared to its diffusion reaction rate, we first consider a model problem that has no mobile ions except the neutral, reactive substrates in the solvent. Fig. 3 *a* shows the reaction rate coefficients with different substrate sizes. It is observed that the rate coefficient increases with the substrate size. This can be explained as follows: the rate is only determined by the diffusion term $a_{33}\nabla p_3$ (see the Supporting Material), due to the zero electric field in this case. Referring to Eq. S5 in the Supporting Material and assuming a constant density, an increase of the substrate size a_3 will lead to an increase of a_{33}, hence giving rise to an increased flux and reaction rate. When the substrate size is changed, its density p will also be adjusted accordingly, but this can be expected to balance only part of the above-described effect to increase the reaction rate.

For the electro-diffusion case in an ionic solution, the reaction rate prediction is complicated by many factors as described in the SMPNP model. Fig. 3 *b* shows the reaction rate coefficients predicted by the SMPNP model. With the simulation conditions described in Fig. 3, at a low concentration of substrate the rate coefficient is also found to increase when the substrate size increases. Because we use a sink boundary condition ($p_3 = 0$) for the reactive substrate, it can be expected that at the molecular boundary the flux is mostly contributed by the diffusion term rather than the drift

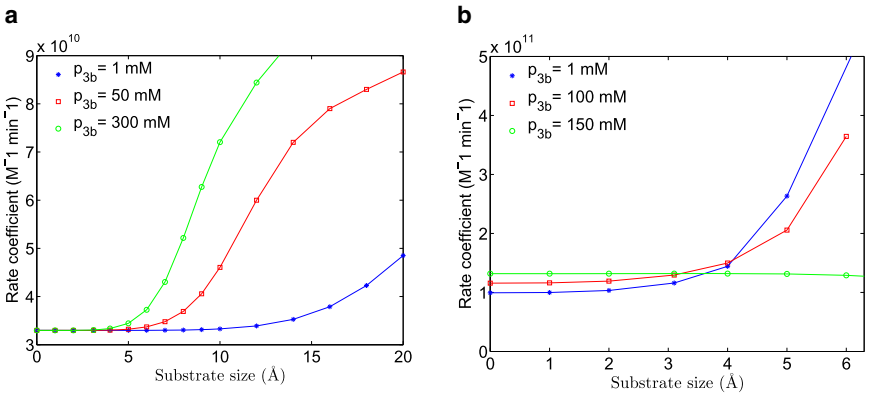

FIGURE 3 Reaction rate coefficients for the sphere model predicted by SMPNP model with different substrate sizes. p_{3b} is the substrate bulk density. (*a*) Substrate alone is diffusive and all particles are electrically neutral. (*b*) Counterion and coion sizes are 3.0 Å, and ionic strength is 150 mM in all SMPNP calculations.

term (proportional to density). Therefore, a significantly increased density gradient should occur when substrate size is considerably enlarged. This can be seen later in Fig. 5 *a*, where the substrate atmosphere is found to be more crowded for large-sized substrates. This seems to contradict the SMPB predictions in which the density for larger sizes should be reduced due to volume exclusion.

As shown in the above subsection, in PB or SMPB, the counterion density near the sphere is high and is three or more orders-larger than the coion density, therefore, its density is sensitive to the size effects. Whereas the coion density is small ($\sim e^{-\beta e\phi}$, ϕ ~4 kcal/mol/e), and similarly the substrate density in SMPNP is usually also small due to depletion, it makes them less sensitive to volume exclusion effects. Differently from the coion case, however, the electric force is attractive to substrate (only the typical attractive case is studied in this work) such as for a counterion, though its density is small near the sphere. Therefore, as expected, a small change in the potential may cause significant variation in the (small) substrate density in the vicinity of the sphere. This is the usual case for the substrate density change in SMPNP modelings, as will be explained below.

The modified potential profile for different size sets is shown in Fig. 4. Due to the volume exclusion of ions and substrate, the solvent occupancy is reduced, and another important factor is that the counterion density is also remarkably reduced; see Fig. 5 *b*. (Note that the coion density is not shown in the figure because it is not sensitive to size effects for the same reason as discussed in SMPB results, above.) These factors contribute to a reduced screening of the electric field, hence to a higher potential. Because the electric force is attractive to substrate, its density is increased near the sphere, which in turn reduces the screening effect again (because of less solvent, and more substrate particles serving as counterions). The larger size then results in higher elevation of the potential near the sphere.

However, in cases that the substrate density in the vicinity of the sphere is large enough, it can also be expected that the volume exclusion itself will appear to take considerable effect to negate its density and density gradient. This factor may balance, or over-balance, the above-described effects. The green line in Fig. 3 *b*, which corresponds to the case of counterion-free and maximum substrate bulk density, shows a slightly decreased reaction rate when the substrate size was increased.

CONCLUSIONS AND DISCUSSION

We demonstrate that the general SMPNP model from the generalized Borukhov free energy functional is a simple and numerically tractable model. In particular, as a special case, an SMPB model for an arbitrary number of different-sized ion species can be achieved through the solution of the SMPNP model by appropriately controlling the boundary/interface conditions. The general SMPNP model can reproduce the main features of the SMPB and SMPNP models that are limited to identical-sized or two-sized

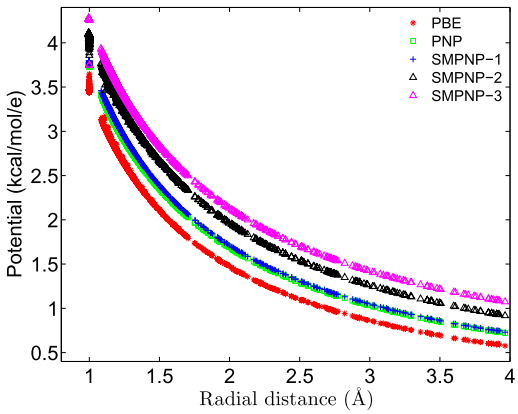

FIGURE 4 Effects of the finite particle sizes on the electrostatic potential in SMPNP. Ionic strength is 150 mM and substrate bulk density is 100 mM in both PNP and SMPNP calculations. In SMPNP-1, the sizes are 3.0, 3.0, and 3.0 $\mathring{A}$ for coion, counterion, and substrate, respectively. In SMPNP-2, these values are 3.0, 5.0, and 5.0 Å; and in SMPNP-3, they are 3.0, 3.0, and 8.0 Å, respectively. The x axis is truncated at $r = 4$ Å in the illustration.

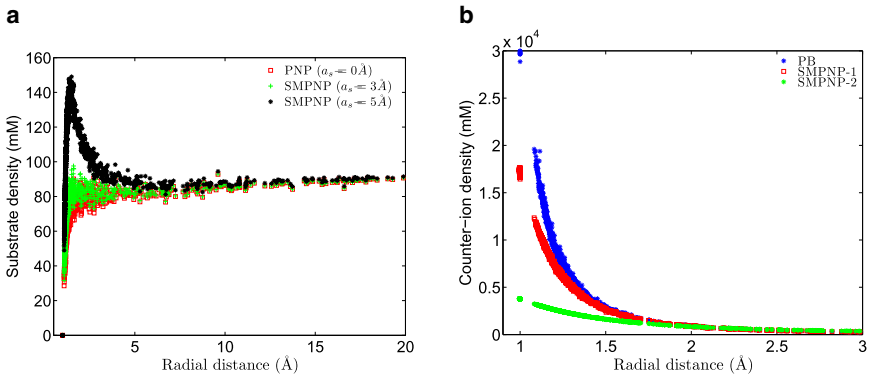

FIGURE 5 Effects of the finite particle sizes on substrate and counterion densities. (*a*) The value a_s is the size of the substrate. All ion sizes are set to 3.0 Å in the SMPNP models. The bulk ionic strength is 150 mM, and bulk substrate density is 100 mM. (*b*) In SMPNP-1, the sizes for coion, counterion, and substrate are 3.0, 3.0, and 3.0 Å, respectively; In SMPNP-2, these sizes are 3.0, 5.0, and 5.0 Å. The bulk densities are the same as in panel *a*. For comparison, the ionic strength is set to 50 mM in the PB calculation because in such cases the counterion bulk density is the same as in the SMPNP case (coion bulk density is 150 mM, substrate bulk density 100 mM, counterion bulk density 50 mM).

species. Our model is applied to the study of diffusion-reaction processes with complicated combinations of sizes of involved particles in practical ionic solution.

It is observed from numerical simulations that the size effects in SMPNP effectively reduce the densities of highly concentrated counterions, as it did in previous MPB models. In the diffusion-reaction simulations, it is found that when the substrate density is very low near the enzyme reactive surface, the predicted reaction rate coefficient of the attractive substrate is larger compared to the results from PNP model, due to volume exclusions of ions and substrate. In the same situation, the substrate density is also observed to be increased near the reactive boundary. This increase is more pronounced when the substrate molecule becomes larger than the solvent molecule.

Plenty of possibilities can be envisioned to improve the current SMPNP model, to improve its numerical treatments, and to promote its applications to biology. The particle sizes in the SMPNP model should be considered as adjustable parameters whose values do not necessarily correspond to the doubling of the particles' van der Waals radii. For instance, a rough estimation of water molecule size a in standard state using the relation between density and size $\rho = 1/a^3$ seems to give $a \sim 11$ Å, which is not the value used in the test examples of this work. When applied to real biological systems, an extensive exploration (such as comparison with experiments and/or explicit molecular dynamics simulations) needs to be done for parameterization for the size values of different ion species and solvent molecules, as was performed by Chu et al. (24). Furthermore, our model considers the particle finite size effects by introducing a penalty term in the free energy functional to model the steric packing. As indicated in previous studies, this term may not be sufficient to describe the more general ion-ion correlations that would involve highly charged molecules and/or multivalent ions.

Recent studies with explicit ion simulations (8) or explicit counterion simulations (51) show that there are noticeable differences between the predicted ion concentrations by the complete continuum models and those by the discrete models. These results also show that certain counterion peak densities can be found significantly reduced in the explicit ion simulation compared with that of the implicit PB simulations (see Fig. 10 *c* in Prabhu et al. (8)), which could be at least partially attributed to the finite size effects. However, alternative scenarios do exist; for instance, it is found that at low ionic strength, the sodium ion concentration in the major groove of the nucleic acid predicted by the explicit ion simulation is higher than that predicted by the PB simulations (8). This indicates that the finite size effects in our PB model can reasonably prevent overestimation for the highly concentrated, saturated ionic profile, but may be insufficient to capture the quantitative features of the ion distribution at low salt concentration when discrete ion effects become dominant.

In this regard, hybrid implicit solvent and explicit ion/particle representations, such as that in Prabhu et al. (8), can be practical treatments for directly capturing the discrete properties. The PNP-like models combined with more-sophisticated DFT theories (27–29) are also feasible strategies to use within the extended PNP framework. Recent work by Eisenberg et al. (1) uses a unified energy variational method by combining the macroscopic (hydrodynamic) and microscopic (atomic) energy functionals to deal with complex ionic solutions; ionic specificity of some one-dimensional ion channels is successfully reproduced (1) (B. Eisenberg, unpublished). In these work, the finite size effects of ions are included either by a Lennard-Jones repulsive term or by a hard sphere term in DFT. Functional integrals will be incurred when using the ion-ion Lennard-Jones interaction to account for the volume exclusion effects of ions. If one considers only the ion-solute Lennard-Jones interactions but neglects the volume exclusion between ions, a system of differential equations can again be obtained (52).

Finally, the complicated system of nonlinear partial differential equations resulting from the SMPNP model poses a serious challenge in numerical solution. It is found that with the method described in this work, the convergence becomes slow for large particle sizes and large biomolecular systems such as the acetylcholinesterase system that we

studied before. Further study in this direction, as well as a speeding-up of the solution by parallel computing, is underway and will be reported upon in future articles.

SUPPORTING MATERIAL

Two additional sections, 18 equations, and one figure are available at http://www.biophysj.org/biophysj/supplemental/S0006-3495(11)00417-6.

The authors are grateful to the reviewers for their helpful comments.

B.L. is partially funded by the Chinese Academy of Sciences, the State Key Laboratory of Scientific and Engineering Computing, and National Science Foundation of China (NSFC grant No. 10971218). Y.C.Z. is supported by Colorado State University.

REFERENCES

1. Eisenberg, B., Y. Hyon, and C. Liu. 2010. Energy variational analysis of ions in water and channels: field theory for primitive models of complex ionic fluids. *J. Chem. Phys.* 133:104104.
2. Barthel, J. M., H. Krienke, and W. Kunz. 1998. Physical Chemistry of Electrolyte Solutions: Modern Aspects. Springer, New York.
3. Fawcett, W. R. 2004. Liquids, Solutions, and Interfaces: From Classical Macroscopic Descriptions to Modern Microscopic Details. Oxford University Press, New York.
4. Fraenkel, D. 2010. Simplified electrostatic model for the thermodynamic excess potentials of binary strong electrolyte solutions with size-dissimilar ions. *Mol. Phys.* 108:1435–1466.
5. Lee, L. L., and R. Lee. 2008. Molecular Thermodynamics of Electrolyte Solutions. World Scientific, Singapore.
6. Gueron, M., and G. Weisbuch. 1979. Polyelectrolyte theory. 2. Activity coefficients in Poisson-Boltzmann and in condensation theory. The polarizability of the counterion sheath. *J. Phys. Chem.* 83:1991–1998.
7. Chu, V. B., Y. Bai, …, S. Doniach. 2008. A repulsive field: advances in the electrostatics of the ion atmosphere. *Curr. Opin. Chem. Biol.* 12:619–625.
8. Prabhu, N. V., M. Panda, …, K. A. Sharp. 2008. Explicit ion, implicit water solvation for molecular dynamics of nucleic acids and highly charged molecules. *J. Comput. Chem.* 29:1113–1130.
9. Durand-Vidal, S., J.-P. Simonin, and P. Turq. 2000. Electrolytes at Interfaces. Kluwer, Boston, MA.
10. Pitzer, K. S. 1991. Activity Coefficients in Electrolyte Solutions, 2nd Ed. CRC Press, Boca Raton, FL.
11. Pitzer, K. S. 1995. Thermodynamics, 3rd Ed. McGraw-Hill College, New York.
12. Pitzer, K. S., and J. J. Kim. 1974. Thermodynamics of electrolytes. IV. Activity and osmotic coefficients for mixed electrolytes. *J. Am. Chem. Soc.* 96:5701–5707.
13. Roger, G. M., S. Durand-Vidal, …, P. Turq. 2009. Electrical conductivity of mixed electrolytes: modeling within the mean spherical approximation. *J. Phys. Chem. B.* 113:8670–8674.
14. Stell, G., and C. G. Joslin. 1986. The Donnan equilibrium: a theoretical study of the effects of interionic forces. *Biophys. J.* 50:855–859.
15. Vrbka, L., M. Lund, …, W. Kunz. 2009. Ion-specific thermodynamics of multicomponent electrolytes: a hybrid HNC/MD approach. *J. Chem. Phys.* 131:154109.
16. Vrbka, L., J. Vondrásek, …, P. Jungwirth. 2006. Quantification and rationalization of the higher affinity of sodium over potassium to protein surfaces. *Proc. Natl. Acad. Sci. USA.* 103:15440–15444.
17. Outhwaite, C. W., L. B. Bhuiyan, and S. Levine. 1980. Theory of the electric double-layer using a modified Poisson-Boltzmann equation. *J. Chem. Soc., Faraday Trans. II.* 76:1388–1408.
18. Rosenfeld, Y., M. Schmidt, …, P. Tarazona. 1997. Fundamental-measure free-energy density functional for hard spheres: dimensional crossover and freezing. *Phys. Rev. E Stat. Phys. Plasmas Fluids Relat. Interdiscip. Topics.* 55:4245–4263.
19. Kraljiglic, V., and A. Iglic. 1994. Influence of finite size of ions on electrostatic properties of electric double layer. *Electrotechnol. Rev. (Slovenia).* 61:127–133.
20. Tang, Z. X., L. E. Scriven, and H. T. Davis. 1994. Effects of solvent exclusion on the force between charged surfaces in electrolyte solution. *J. Chem. Phys.* 100:4527–4530.
21. Coalson, R. D., A. M. Walsh, …, N. Ben-Tal. 1995. Statistical mechanics of a Coulomb gas with finite size particles: a lattice field theory approach. *J. Chem. Phys.* 102:4584–4594.
22. Borukhov, I., D. Andelman, and H. Orland. 1997. Steric effects in electrolytes: a modified Poisson-Boltzmann equation. *Phys. Rev. Lett.* 79:435–438.
23. Antypov, D., M. C. Barbosa, and C. Holm. 2005. Incorporation of excluded-volume correlations into Poisson-Boltzmann theory. *Phys. Rev. E Stat. Nonlin. Soft Matter Phys.* 71:061106.
24. Chu, V. B., Y. Bai, …, S. Doniach. 2007. Evaluation of ion binding to DNA duplexes using a size-modified Poisson-Boltzmann theory. *Biophys. J.* 93:3202–3209.
25. Kilic, M. S., M. Z. Bazant, and A. Ajdari. 2007. Steric effects in the dynamics of electrolytes at large applied voltages. II. Modified Poisson-Nernst-Planck equations. *Phys. Rev. E Stat. Nonlin. Soft Matter Phys.* 75:021503.
26. Kalcher, I., J. C. F. Schulz, and J. Dzubiella. 2010. Ion-specific excluded-volume correlations and solvation forces. *Phys. Rev. Lett.* 104:097802.
27. Gillespie, D., W. Nonner, and R. S. Eisenberg. 2002. Coupling Poisson-Nernst-Planck and density functional theory to calculate ion flux. *J. Phys. Condens. Matter.* 14:12129–12145.
28. Gillespie, D., W. Nonner, and R. S. Eisenberg. 2003. Density functional theory of charged, hard-sphere fluids. *Phys. Rev. E Stat. Nonlin. Soft Matter Phys.* 68:031503.
29. Gillespie, D., M. Valiskó, and D. Boda. 2005. Density functional theory of the electrical double layer: the RFD functional. *J. Phys. Condens. Matter.* 17:6609.
30. Evans, R. 1992. Density functionals in the theory of nonuniform fluids. *In* Fundamentals of Inhomogeneous Fluids. D. Henderson, editor. Marcel Dekker, New York. 606.
31. Roth, R., R. Evans, …, G. Kahl. 2002. Fundamental measure theory for hard-sphere mixtures revisited: the White Bear version. *J. Phys. Condens. Matter.* 14:12063.
32. Hansen-Goos, H., and R. Roth. 2006. Density functional theory for hard-sphere mixtures: the White Bear version Mark II. *J. Phys. Condens. Matter.* 18:8413.
33. Rosenfeld, Y. 1996. Geometrically based density-functional theory for confined fluids of asymmetric ("complex") molecules. *In* Chemical Applications of Density-Functional Theory. B. B. Laird, R. B. Ross, and T. Ziegler, editors. American Chemical Society, Washington, DC. 198–212.
34. Roth, R. 2010. Fundamental measure theory for hard-sphere mixtures: a review. *J. Phys. Condens. Matter.* 22:063102.
35. Kunz, W., and R. Neueder. 2009. An attempt at an overview. *In* Specific Ion Effects. W. Kunz, editor. World Scientific Publishing Company, Singapore. 11–54.
36. Eigen, M., and E. Wicke. 1954. The thermodynamics of electrolytes at higher concentration. *J. Phys. Chem.* 58:702–714.
37. Rutkai, G., D. Boda, and T. Kristóf. 2010. Relating binding affinity to dynamical selectivity from dynamic Monte Carlo simulations of a model calcium channel. *J. Phys. Chem. Lett.* 1:2179–2184.
38. Boda, D., W. Nonner, …, D. Gillespie. 2007. Steric selectivity in Na channels arising from protein polarization and mobile side chains. *Biophys. J.* 93:1960–1980.

39. Gillespie, D., and D. Boda. 2008. The anomalous mole fraction effect in calcium channels: a measure of preferential selectivity. *Biophys. J.* 95:2658–2672.

40. Boda, D., M. Valiskó, …, W. Nonner. 2009. Ionic selectivity in L-type calcium channels by electrostatics and hard-core repulsion. *J. Gen. Physiol.* 133:497–509.

41. Reference deleted at proof.

42. Lu, B.Z., Y.C. Zhou, …, J.A. McCammon. 2008. Size-modified continuum model. Progress report by the McCammon group at the University of California at San Diego, June 2008, CTBP Summer School "Coarse-Grained Physical Modeling of Biological Systems: Advanced Theory and Methods".

43. Lu, B. Z., Y. C. Zhou, …, J. A. McCammon. 2007. Electrodiffusion: a continuum modeling framework for biomolecular systems with realistic spatiotemporal resolution. *J. Chem. Phys.* 127:135102.

44. Lu, B. Z., M. J. Holst, …, Y. C. Zhou. 2010. Poisson-Nernst-Planck equations for simulating biomolecular diffusion-reaction processes. I: Finite element solutions. *J. Comput. Phys.* 229:6979–6994.

45. Burak, Y., and D. Andelman. 2000. Hydration interactions: aqueous solvent effects in electric double layers. *Phys. Rev. E Stat. Phys. Plasmas Fluids Relat. Interdiscip. Topics.* 62(4 Pt B):5296–5312.

46. Grochowski, P., and J. Trylska. 2008. Continuum molecular electrostatics, salt effects, and counterion binding—a review of the Poisson-Boltzmann theory and its modifications. *Biopolymers.* 89:93–113.

47. Li, B. 2009. Continuum electrostatics for ionic solutions with nonuniform ionic sizes. *Nonlinearity.* 22:811–833.

48. Bank, R. E., D. J. Rose, and W. Fichtner. 1983. Numerical methods for semiconductor device simulation. *SIAM J. Sci. Statist. Comput.* 4:416–435.

49. Jerome, J. W. 1996. Analysis of Charge Transport: A Mathematical Study of Semiconductor Devices. Springer, New York.

50. Gatti, E., S. Micheletti, and R. Sacco. 1998. A new Galerkin framework for the drift-diffusion equation in semiconductors. *East-West. J. Numer. Math.* 6:101–135.

51. Ye, X., Q. Cai, …, R. Luo. 2009. Roles of boundary conditions in DNA simulations: analysis of ion distributions with the finite-difference Poisson-Boltzmann method. *Biophys. J.* 97:554–562.

52. Lu, B. Z., and J. A. McCammon. 2008. Molecular surface-free continuum model for electrodiffusion processes. *Chem. Phys. Lett.* 451:282–286.

Poisson-Nernst-Planck Equations for Simulating Biomolecular Diffusion-Reaction Processes II: Size Effects on Ionic Distributions and Diffusion-reaction Rates

(Supplementary Material)

Benzhuo Lu, and Y. C. Zhou

S1 Numerical implementation of the SMPNP equations

S1.1 The free energy functional is convex

We will first show that the free energy functional 24 of the SMPNP system is convex. Since ϕ is determined by the ion densities through the PE

$$\rho = L\phi,$$

we note the dependence of ϕ on p as $\phi[p] = L^{-1}\rho$, where $\rho = \rho^f + \lambda\sum_i z_i e p_i$ is the total charge density, and $L = -\nabla\cdot\varepsilon\nabla$ is the partial differential operator corresponding to the Poisson equation. By taking the first-order variation of the functional 24 with respect to δp_i we get

$$(\delta F[p])_i = \int \left[q_i\phi + k_B T \ln(p_i a_i^3) - k_B T a_0^{-3} a_i^3 \ln(1 - \sum_l^K a_l^3 p_l) - \mu_i \right] \delta p_i dx. \quad \text{(S1)}$$

The second order functional variation with respect to δp_j is

$$(\delta F[p])_{i,j} = \int \left[q_i \delta p_i (L^{-1} q_j \delta p_j) + k_B T \frac{\delta_{ij}\delta p_i \delta p_j}{p_i} + k_B T a_0^{-3} \frac{a_i^3 a_j^3 \delta p_i \delta p_j}{1 - \sum_l^K a_l^3 p_l} \right] dx. \quad \text{(S2)}$$

It is known that that the elliptic operator L (hence L^{-1}) is definite positive because ε is piecewise constant. Let H be the Hessian $\frac{\delta^2 F[p]}{\delta p_i \delta p_j}$. For any non-zero variation in densities p (densities are always positive $p_i > 0$), i.e. $p \to p + \delta p$,

$$\delta p \cdot H \delta p = \int \left[(\sum_i^K q_i \delta p_i)(L^{-1} \sum_i^K q_i \delta p_i) + \sum_i^K k_B T \frac{(\delta p_i)^2}{p_i} + k_B T \frac{a_0^{-3} (\sum_i^K a_i^3 \delta p_i)^2}{1 - \sum_l^K a_l^3 p_l} \right] dx$$
$$\geqslant 0. \quad \text{(S3)}$$

Therefore, H is symmetric, semi-positive definitive. It follows that $F[p]$ is convex. This guarantees a unique solution for the SMPNP equations. This fact will be used in the subsection 2.4 of the paper to make sure that the SMPBE model can be obtained from the solution of the SMPNP equations at certain conditions.

S1.2 Finite element method for the NP equations

We write Eq. 34 in a brief form:

$$-\nabla \cdot J_i = -\nabla \cdot \left[\sum_j a_{ij}(r, p(r)) \nabla p_j(r) + b_i(r) p_i(r)) \right] = 0, \tag{S4}$$

where p represents the vector $\{p_1, p_2, ..p_K\}$. Here and in the sequel, J_i denotes the negation of the real flux j_i of species i, $J_i = -j_i$. The matrix **a** and the vector **b** are given by

$$a_{ij} = \delta_{ij} D_j + \frac{D_i(r) k_i p_i(r) a_j^3}{1 - \sum_l a_l^3 p_l(r)}, \tag{S5}$$

$$b_i = \beta D_i(r) q_i \nabla \phi(r). \tag{S6}$$

The finite element solution strategy for a general coupled non-linear elliptic partial differential equation system is referred to (*S1*). Below we outline the essential ingredients of the FEM solution of the steady state PNP equations S4. We define the solution space

$$H := \left\{ p \in H^1_{0_1}(\Omega_s) \times \cdots H^1_{0_n}(\Omega_s) \right\} \tag{S7}$$

and its finite dimensional subspace

$$S := \left\{ p \in (P_1(\Omega_s))^n \right\}, \tag{S8}$$

where the vector $p = \left\{ p_j \right\}_{j=1}^n$, and P_1 is the space consisting of piecewise linear tetrahedral finite elements. Functions in the space

$$H^1_{0_i} = \left\{ v \in H^1(\Omega_s) : v = 0 \; on \; \partial\Omega, v = 0 \; on \; \Gamma_{D_i} \right\}$$

satisfy the Dirichlet boundary condition on the exterior boundary $\partial\Omega$ and the essential or Dirichlet boundary condition on the molecular surface Γ if there is one. We assume that the finite elements are regular and quasi-uniform. The weak formulation of the problem of the whole PNP system now is:

Find $u = p \in S$ such that

$$\langle F(u), v\rangle = 0, \quad \forall v \in S. \tag{S9}$$

The weak form of Eq. S4 is

$$\langle F(p), v\rangle|_i = \int_{\Omega_s} (J_i \cdot \nabla v_i) dx = \int_{\Omega_s} \left[\sum_j a_{ij}(r,p)\nabla p_j + b_i p_i\right] \cdot \nabla v_i dx \tag{S10}$$

and the Newton-type iterations necessitate its bilinear form defined by the Gâteaux derivative $DF(u)$

$$\begin{aligned}\langle DF(p)w, v\rangle_i &= \frac{d}{dl}\langle F(p+lw), v\rangle_i|_{l=0} \\ &= \int_{\Omega_s} \left[\sum_j a_{ij}\nabla w_j \cdot \nabla v_i + \sum_j \frac{\partial a_{ij}}{\partial p_k} w_k \nabla p_j \cdot \nabla v_i + b_i w_i \cdot \nabla v_i\right] dx,\end{aligned} \tag{S11}$$

where w is functions from the same basis as v.

The derivatives (Gateaux) of a_{ij} are:

$$\frac{\partial a_{ij}}{\partial p_k} = \frac{D_i k_i \delta_{ik} a_j^3}{1 - \sum_l a_l^3 p_l} + \frac{D_i k_i p_i a_k^3 a_j^3}{(1 - \sum_l a_l^3 p_l)^2}. \tag{S12}$$

The first term in Eq. S11 leads to a symmetric stiffness matrix, but the latter two will not.

S1.3 Treatment of singular charges in Poisson equation

Two common issues exist in the solution of biomolecular electrostatic governed by either the PE 5 or the traditional PBE. These are (i) the point charge singularity, (ii) the dielectric discontinuity across a molecular surface. For a rigorous treatment of the singular charges we introduce the Green's function for the Laplace equation and a harmonic function; the summation of these functions amounts to the zeroth order approximation to the solution to solve the point charge singularity problem. The potential is decomposed into three parts $\phi = \phi^s + \phi^h + \phi^r$. It defines a singular potential ϕ^s only in the domain Ω_m,

$$\begin{aligned}\phi^s &= G|_{\overline{\Omega}_m} \text{ in } \overline{\Omega}_m, \\ \phi^s &= 0 \text{ in } \Omega_s,\end{aligned} \tag{S13}$$

where the singular potential G solves $-\varepsilon_m \Delta G = \rho^f$ in $\mathcal{R}^3$, and uses a harmonic component ϕ^h to compensate the discontinuity of ϕ^s on Γ

$$\begin{aligned} \Delta\phi^h &= 0 \text{ in } \Omega_m, \\ \phi^h &= -\phi^s \text{ on } \Gamma. \end{aligned} \tag{S14}$$

Subtracting these two components from the PE 5, one obtains the equation for the regular potential ϕ^r:

$$\begin{aligned} -\nabla\cdot(\varepsilon\nabla\phi^r) - \lambda\sum q_i p_i &= 0 \text{ in } \Omega, \\ [\phi^r] = 0,\ \left[\varepsilon\frac{\partial\phi^r}{\partial n}\right] &= -\varepsilon_m\left(\frac{\partial\phi^s}{\partial n} + \frac{\partial\phi^h}{\partial n}\right) \text{ on } \Gamma. \end{aligned} \tag{S15}$$

Similarly the regular part for the nonlinear PBE satisfies:

$$-\nabla\cdot(\varepsilon\nabla\phi^r) + \kappa^2\sinh(\phi^r) = 0 \text{ in } \Omega. \tag{S16}$$

Numerical experiments illustrating the stable convergence are shown in (*S2*). The weak form, bilinear form, and more details of FEM solution of the PBE can be seen in (44) and (*S3*).

S1.4 Relaxed Gummel iteration for the SMPNP equations

A standard Gummel iteration proceeds as following: given any initial solution function ϕ^0 (or p^0), solve the NP equations Eqs. 34 (or the PE 35) to get a solution p^0 (ϕ^0), then solve the PE (NPEs) with these p^0 (ϕ^0) to get an updated solution ϕ^1 (p^1), and with ϕ^1 get an updated solution of NPEs p^2 (ϕ^2 of the PE), continue this iteration until approaching a converged solution (p,ϕ) of the PE and the NPEs.

It is found that the standard Gummel iteration converges slowly, and may diverge in some circumstances. A γ-iteration procedure for the iteration between the NP and PE as used in our former PNP solution (43) appears also helpful in assisting convergence of solution for our SMPNP system. When obtained a solution (p_n,ϕ_n) of the SMPNP equations at the n-th step during the iterations between solutions of the PE and SM NPEs, we modify them for use in next iteration step by a γ-relaxation

$$p_i^n = \gamma p_i^n + (1-\gamma)p_i^{n-1}, \tag{S17}$$

$$\phi^n = \gamma\phi^n + (1-\gamma)\phi^{n-1}. \tag{S18}$$

It is found that usually under-relaxation, i.e. $\gamma < 1$ is necessary for the SMPNP

system, while over-relaxation does not help the convergence.

S2 Substrate concentration dependency of the rate coefficient

We first perform simulations of the substrate diffusion-reaction process using the PNP model that does not have the size effects. As shown previously (*S4*, *S5*) the rate coefficient is dependent on substrate bulk density, even for a fixed ionic strength (see Fig. S1 for the sphere case). In particular, for attractive substrate, increasing of substrate density can speed up the diffusion process and thus increase the rate coefficient significantly. The sphere model shows the same tendency of the rate-concentration dependence as that in the enzyme model (*S5*) for the similar underlying physics.

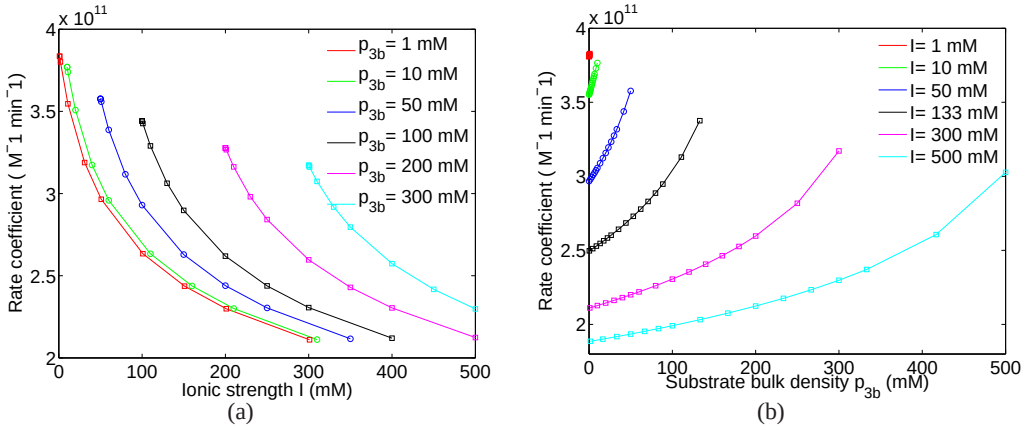

Figure S1: Rate coefficients from PNP model for a spherical case. The bulk ion densities and the substrate density keep charge neutral.

References

[S1] Holst, M., 2001. Adaptive numerical treatment of elliptic systems on manifolds. *Adv. in Comput. Math.* 15:139–191.

[S2] Holst, M., J. A. McCammon, Z. Yu, Y. C. Zhou, and Y. Zhu, 2011. Adaptive finite element modeling techniques for the Poisson-Boltzmann equation. *Commun. Comput. Phys.* In press.

[S3] Lu, B. Z., Y. C. Zhou, M. Holst, and J. A. McCammon, 2008. Recent progress in numerical solution of the poisson-boltzmann equation for biophysical applications. *Commun. in Comput. Phys.* 3:9731009.

[S4] Zhou, Y. C., B. Z. Lu, G. A. Huber, M. J. Holst, and J. A. McCammon, 2008. Continuum simulations of acetylcholine consumption by acetylcholinesterase: A Poisson-Nernst-Planck approach. *J. Phys. Chem. B* 112:270–275.

[S5] Lu, B. Z., and J. A. McCammon, 2010. Kinetics of diffusion-controlled enzymatic reactions with charged substrates. *PMC Biophysics* 3:1.